Compositionally Graded Hydrophobic UV-Cured Coatings for the Prevention of Glass Stress Corrosion

coatings

MDPI

Article

Compositionally Graded Hydrophobic UV-Cured Coatings for the Prevention of Glass Stress Corrosion

Sara Dalle Vacche [1,2,*], Gregorio Mariggiò [3], Alessandra Vitale [1,2], Roberta Bongiovanni [1,2] and Mauro Corrado [3]

1 Department of Applied Science and Technology (DISAT), Politecnico di Torino, Corso Duca degli Abruzzi 24, 10129 Torino, Italy
2 INSTM-Politecnico di Torino Research Unit, 50121 Firenze, Italy
3 Department of Structural, Geotechnical and Building Engineering, Politecnico di Torino, Corso Duca degli Abruzzi 24, 10129 Torino, Italy
* Correspondence: sara.dallevacche@polito.it

Received: 31 May 2019; Accepted: 1 July 2019; Published: 4 July 2019

Abstract: The use of glass in architecture is growing and is moving towards structural applications. However, the tensile strength of glass cannot be fully exploited because of stress corrosion. This is a corrosion triggered by stress applied to the material and dependent on environmental factors such as humidity and temperature. To protect glass from stress corrosion, we developed a UV-cured coating, characterized by hydrophobicity, barrier to water vapor properties, and good adhesion to glass, thanks to a compositional profile. The coating was obtained by combining a cycloaliphatic diacrylate resin with a very low amount of a perfluoropolyether methacrylate co-monomer, which migrated to the free surface, creating a compositionally graded coating. The adhesion to glass was improved, using as a primer an acrylated silane able to co-react with the resins. With a mechanical load test using the coaxial double ring set-up, we proved that the coating is effective in the inhibition of stress corrosion of glass plates, with an increase of 76% of tensile strength.

Keywords: glass stress corrosion; UV-cured coatings; fluorinated acrylate; barrier to water vapor; adhesion

1. Introduction

The use of glass in architecture is growing, not only for grand facades of modern buildings, but also for new structural applications, such as, for instance, glass-made staircases, roofs, load-bearing beams, and walkways [1]. Such challenging applications are pushed forward by the aesthetic value conferred to the material, which allows architects to find innovative and minimalist solutions to fulfill their creative ideas. Moreover, the construction of glass structures saves energy and improves wellbeing, as it maximizes the use of sunlight and exploits insulation properties. Thanks to this trend, the studies in this field are increasing and different solutions for structural application of glass have been found [2,3].

The need to treat glass for load-bearing applications comes from the inherent characteristics of the material, which has well known thermal and chemical properties, but is also very brittle, especially under certain environmental conditions, in which tensile strength of glass cannot be fully exploited. The strength of glass is highly dependent on the condition of its surface. The intrinsic strength of glass is very high and can reach 32 GPa, based on the intermolecular bonds that are developed in the glass molecular network [4]. However, stress-raising flaws (known as Griffith flaws) accumulate on the glass surface as a result of manufacturing, transportation, and surface damage during its service life.

This leads to a significant reduction in tensile strength to a value commonly referred to as the extrinsic strength, which can be computed with linear elastic fracture mechanics based formulas:

$$\sigma_f = \frac{K_{IC}}{Y \cdot \sqrt{\pi \cdot a}} \quad (1)$$

where Y is a geometry factor, dependent on the shape of the crack, a is the crack depth, and K_{IC} is the fracture toughness. The deeper the surface flaws, the lower the extrinsic strength. For example, for a typical half-penny-shaped crack with a = 50 µm on the surface of the glass, K_{IC} = 0.75 MPa·m$^{0.5}$ and Y = 0.713, the extrinsic strength, computed with Equation (1), is reduced to σ_f = 76.7 MPa. The evaluation of the correct value of fracture toughness, together with the definition of the geometry factor Y, is, therefore, of paramount importance for the prediction of failure of the glass components. As such, it has been the object of several studies [5–8]. In particular, in ref. [8], two important techniques for the evaluation of fracture toughness at the micro-scale are reviewed: The pillar splitting method, based on a sharp nanoindentation, which is particularly useful for testing of thin ceramic films; and the micro-cantilever method, which is suitable for the analysis of fracture mechanisms in brittle and semi-brittle materials. Besides its brittleness and sensitivity to cracks and flaws, glass is affected by stress corrosion, a degradation phenomenon that is due to the subcritical growth of surface flaws and microcracks, with a consequent decrease of the tensile strength of the material over time [9]. The stress corrosion mechanism depends on intrinsic factors as size and shape of surface flaws and external variables, namely environmental conditions and applied loads [10,11]. Currently, different studies agree that the presence of water favors the growth of micrometric surface defects and cracks. Water molecules cause chemical reactions that depend on the composition of glass (Figure 1), which bring about the rupture of silicon–oxygen bonds [12]; the activation energy for these reactions is provided by external stress [13]. Different ways to overcome stress corrosion have been found; so far, the well-known solutions for glass strengthening are based on tempering processes, either through thermal or chemical treatments, which produce a surface compression state [14]. However, there are different issues with these technologies, such as high-energy costs and/or long treatment times [15].

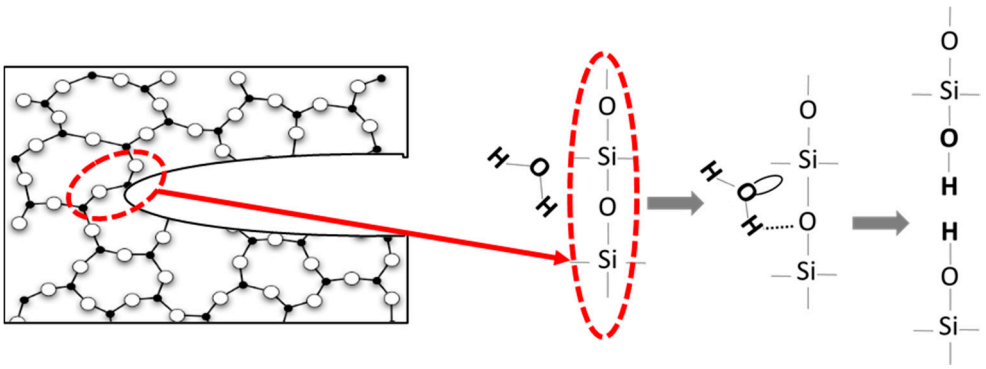

Figure 1. Stress corrosion reaction mechanism at the tip of a crack. Reaction steps involve: Adsorption of water to silicon–oxygen (Si–O) bond, concerted reaction involving simultaneous proton and electron transfer, and formation of surface hydroxyl groups.

The application of a protective polymeric coating can be an alternative. Such coatings have the advantage of limiting the intervention to the surfaces of the glass plates, while maintaining the transparency of the structural component. Moreover, they are routinely used in the glass industry for many purposes; selective coatings to improve the thermal performance of glazing, anti-fingerprint coatings, and anti-shatter films are just a few examples [16]. In most cases, UV-cured coatings are preferred because they are environmentally friendly: They do not contain solvents and, therefore, toxic organic-vapor emissions are minimized. In addition, costs are reduced because the polymerization takes place in a few seconds and does not require heating. Typically, UV-cured coatings are made of

acrylates, a class of polymers characterized by a high reaction rate, stability, and high glass transition temperature, which makes them more resistant and suitable for outdoor applications [17]. However, they have poor adhesion and do not show water repellency, which are properties required for protecting glass from stress corrosion. The use of fluoropolymers is well known for water resistance and water repellency [18], while silanes can ensure adhesion, acting as a bridge and creating covalent bonds between the polymer and the glass surface [19,20]. Preferably, a glass coating against stress corrosion must maximize adhesion on the glass side and hydrophobicity on the air side.

Therefore, in this work we examine a UV-curable acrylic system copolymerized with a methacrylic perfluoropolyether (PFPE) and an acrylic silane. The challenge was to obtain the best balance between hydrophobicity and adhesion of the coating, which are usually in competition. The composition of the coating was chosen with the aim of developing a copolymer exhibiting a compositional gradient, so that the obtained coating ensured water repellency, thanks to the surface segregation of the fluorinated component, and adhesion towards the glass substrate, thanks to the presence of the silane at the interface. Concerning the selection of the fluorinated co-monomer, attention was paid to the present constraints and regulations on the use of this class of chemicals. In fact, fluoroalkylic chains of type C_nF_{2n+1} raise concerns for being toxic, persistently polluting the environment and bioaccumulating in humans. Short-chain fluorinated chains (i.e., shorter than C_4) and perfluoropolyethers are considered safe alternatives, approved by the U.S. Food & Drugs Administration (FDA) and the European Food Safety Authority (EFSA) [21,22]. We investigated the adhesive bond strength of the coating and its resistance to water, and we tested the coating effectiveness in stress corrosion prevention with quasi-static mechanical tests, performed with the coaxial double ring setup.

2. Materials and Methods

2.1. Materials

The chemical structures of the products used in this work are reported in Figure 2.

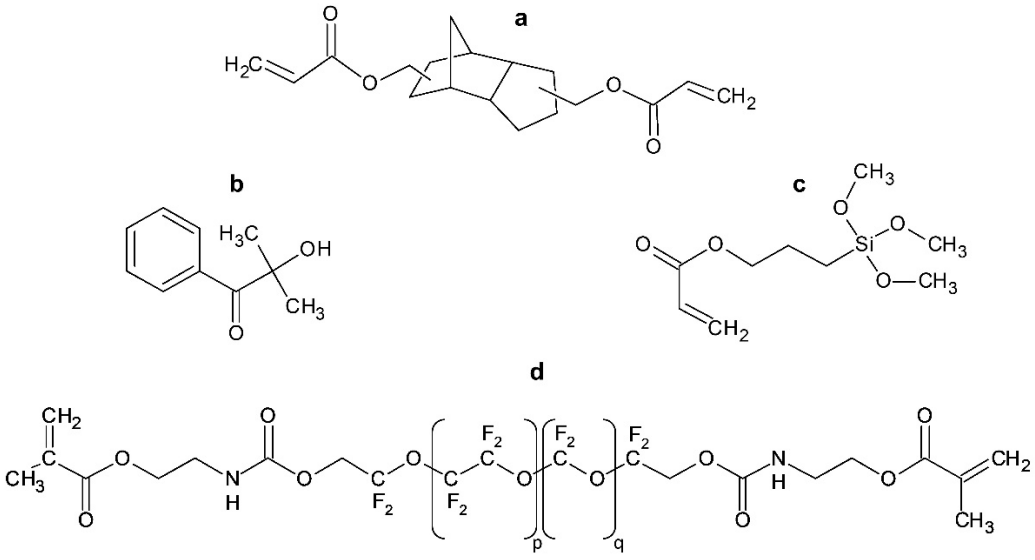

Figure 2. Chemical structures of (**a**) Ebecryl® 130 (E), (**b**) Darocur® 1173 (D), (**c**) 3-(acryloyloxy) propyltrimethoxysilane, and (**d**) Fluorolink® MD700 (F).

Tricyclodecanediol diacrylate (Ebecryl® 130, by Allnex Belgium SA, Drogenbos, Belgium) and a bifunctional urethane methacrylate perfluoropolyether (PFPE) macromer containing more than 80% of PFPE (Fluorolink® MD700, by Solvay Specialty Polymers, Bollate Milano, Italy) were used as oligomers, and will be called "E" and "F", respectively, in what follows. We added 2-hydroxy 2-methyl 1-phenyl propan-1-one (Darocur® 1173, by BASF, Ludwigshafen, Germany), henceforth indicated with

D, as a photoinitiator; the silane was 3-(acryloyloxy) propyltrimethoxysilane, 94%, supplied by Alfa Aesar (Thermo Fisher (Kandel) GmbH, Karlsruhe, Germany).

Thermo Scientific™ British standard slides (referred to as "glass slide" in what follows) made from extra-white soda-lime glass, (Thermo Fisher Scientific Inc., Waltham, MA, USA) were used as substrates for the coating characterization. Soda-lime glass square plates with side D = 120 mm and thickness h = 4 mm (referred to as "glass plates") were used for loading tests.

2.2. Silanization of Glass Slides

Silanization of glass with 3-(acryloyloxy) propyltrimethoxysilane was carried out following the procedure reported in ref. [23]. Glass substrates were surface-modified by immersion in ethanol or water solutions of the silane. The concentration of silane was 0.2 vol.% and 1 vol.% in ethanol and 0.2 vol.% in water. For both water-based and ethanol-based silanization, treated slides and plates were dried in an oven at 115 °C for 1 h to promote silanol condensation.

2.3. Preparation of Test Specimens

The composition of the coating investigated in this work is summarized in Table 1. In the following, it is referred to as "EFD", from the codes of its constituents.

Table 1. Composition of the coating EFD.

Product	Code	phr
Ebecryl® 130	E	100
Fluorolink® MD700	F	1
Darocur® 1173	D	3

Reference coatings were made using 100 phr of E or F, combined with 3 phr of photoinitiator D—they are labelled ED and FD, respectively.

For each characterization test, a specific protocol for the sample preparation was followed.

- Specimens for water contact angle, resistance to water, UV-visible spectroscopy, and coaxial double ring test: Coatings with 50 μm thickness were prepared on glass substrates using a wire bar coater. The wettability of the substrates was tested before use to check for the presence of contaminants. The glass plates used for the load test were washed with water and soap, while glass slides were used as received.
- Specimens for single lap shear test: Surface-modified glass slides were used, with a circular bonding area having a diameter of 4 mm. The procedure sketched in Figure 3 was adapted from Swentek and Wood [24]. A polytetrafluoroethylene (PTFE) mask (100 μm thick), slightly larger than the overlapped area of the two slides, was punched to obtain a circular hole; four perpendicular cuts were pre-made on the PTFE mask in order to ease removal after the curing. The mask was placed on one glass slide and the correct amount of resin was placed into the circular hole with a syringe, then a second glass slide was placed on top. The joint was then cured as described below, and the mask was removed by tearing it apart. Other glass slides were used as spacers for the alignment of the specimens, both during assembly and in the dynamometer.
- Specimens for water vapor permeability tests: A 100 μm wire bar coater was used to prepare the films.

All types of specimens were cured with a 5000-EC UV flood lamp system (Dymax Corporation, Torrington, CT, USA) with a medium intensity mercury bulb. The intensity of the radiation was measured by means of a UV Power Puck II radiometer (EIT, LLC., Leesburg, VA, USA) and was tuned by changing the distance between the specimens and the UV source. The coatings were cured with an intensity of 100 mW·cm^{-2} for 2 min under N_2 flow, after 30 s of N_2 flow prior to curing. The lap shear specimens were cured at 100 mW·cm^{-2} intensity in air for 3 min (1.5 min per side).

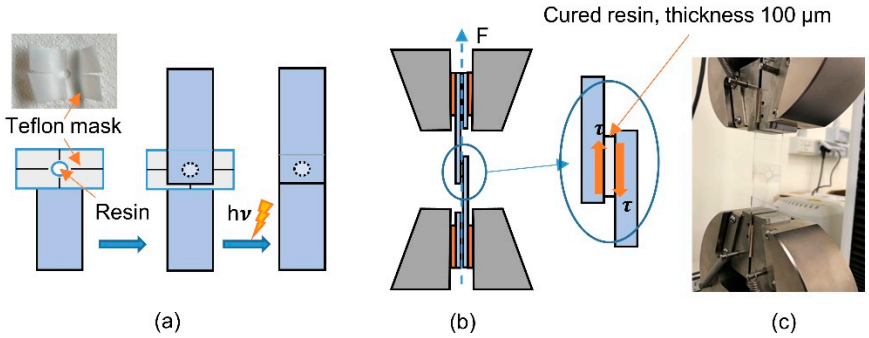

Figure 3. (**a**) Scheme of the preparation of the single lap shear specimen and photo of the polytetrafluoroethylene (PTFE) mask; (**b**) scheme of the lap shear specimen mounted in the tensile test set-up; (**c**) photo of a cured specimen in the tensile set up.

2.4. Characterization Methods

Static contact angle measurements were performed in order to assess the surface properties of both glass and coatings. A Krüss DSA100 instrument (KRÜSS GmbH, Hamburg, Germany) was used, equipped with video camera and image analysis software, with the sessile drop technique. Water and hexadecane were the testing liquids and each measurement was repeated five times. Water and hexadecane drops were 10 and 5 µL, respectively. Contact angle measurements were used to estimate the surface energy of the coating, according to the geometric average model [25]:

$$(1 + \cos\theta_i)\cdot\gamma_i = 2\cdot\left[\left(\gamma_i^D\cdot\gamma_s^D\right)^{1/2}\cdot\left(\gamma_i^P\cdot\gamma_s^P\right)^{1/2}\right] \quad (2)$$

$$\gamma_s = \gamma_s^D + \gamma_s^P \quad (3)$$

where θ_i is the contact angle measured on the solid for the liquid i (water or hexadecane); γ_s, γ_s^D, and γ_s^P indicate the surface energy of the solid surface (polymer), and its dispersive and polar components, respectively. The surface energy values used for the calculations, embedded in the internal library of the FTA32 Software (version 2.1, First Ten Ångstroms, Portsmouth, VA, USA), are for water, γ_w = 72.8 mN·m^{-1}, γ_w^D = 21.8 mN·m^{-1}, γ_w^P = 51.0 mN·m^{-1}, and for hexadecane, γ_h = 28.1 mN·m^{-1}, γ_h^D = 28.1 mN·m^{-1}, γ_h^D = 0 mN·m^{-1}. Water contact angle analyses were repeated after the lap shear mechanical tests on the site of detachment of the joints. In this case, due to the small area of interest, only one measurement per sample was performed.

The surface roughness of bare and coated glass slides was assessed with a Surftest 201 series 178 portable measuring instrument (Mitutoyo Italiana S.r.L., Lainate, Italy), according to DIN 4768 standard [26]. The sampling length was set at 0.8 mm and the evaluation length was taken as three times the sampling length. The arithmetic average roughness R_a, the mean roughness depth R_z, and the maximum roughness depth R_{max} were reported.

A JENWAY 6850 UV/Vis (Cole-Parmer, Stone, UK) UV-visible spectrophotometer was used to evaluate the transparency of the coatings; standard British glass slides were used as reference.

Resistance to water was assessed by immersion of the coated glass in demineralized water for 14 days at room temperature (RT), followed by 4 h at 60 °C. Daily inspections were performed according to the ASTM D870-15 (2015) standard [27].

Gloss values were measured with a ZGM 1020 glossmeter with a 60° angle (P. Zehtner Testing Instruments, Reigoldswil, Switzerland). A glass slide was taken as reference, and the relative change in gloss due to the coating was evaluated.

Single lap shear tests were performed by means of an Instron 3366 electromechanical universal testing machine (ITW Test and Measurement Italia S.r.l. Instron CEAST Division, Pianezza, Italy) equipped with a 10 kN load cell. Six specimens were tested with a cross head speed of 5 mm/min; the adhesive strength of the joint, τ_{max}, was calculated as the ratio between the maximum load F_{max}

obtained during the lap shear test and the initial bonded area A, which was calculated from the diameter of the PTFE mask's circular hole.

A MultiPerm permeometer (ExtraSolution made by PermTech, Pieve Fosciana, Italy) was used to measure the Water Vapor Transmission Rate (WVTR). The test conditions were adapted from the ASTM F372-99 (2003) standard [28]; relative humidity was set at 80%. WVTR of each coating was evaluated as the average of three measurements and compared to a standard 25 μm PET film, used as a reference for barrier to water properties. All the specimens were subjected to a conditioning cycle to remove the residual humidity from the chambers and the films, bringing the system to the set temperature. The duration of the conditioning cycle was 15 h. All the WVTR results were normalized to a thickness of 25 μm, according to Equation (4):

$$\mathrm{WVTR}_{25} = \frac{\mathrm{WVTR} \cdot l}{25} \tag{4}$$

where l is the thickness of the film in μm. Specimen thickness was measured with a coating thickness gauge QuaNix 7500 (Automation USA, Westminster, CA, USA). An optical microscope Olympus BX53M (Olympus Corp., Tokyo, Japan) was used to analyze the morphology of the films before and after permeability tests.

Mechanical load tests were performed to verify the effectiveness of the coating in protecting the glass surface against stress corrosion, using the coaxial double ring set-up, according to the ASTM C1499-15 standard (2015) [29]. The specimens were immersed in water during loading tests in order to simulate a harsh environment. As shown in Figure 4, the double ring set-up consists of a pair of steel rings with different diameters: The largest one has a diameter of D_S = 90 mm and supports the specimens, the second one has a diameter of D_L = 40 mm and is used to apply a normal force on the upper surface of the sample producing a bi-axial bending stress state in the plate. A constant stress rate equal to 0.15 MPa·s^{-1} was applied until failure of the plate. The equibiaxial tensile strength was calculated from the maximum load by means of the following equation, taken from the theory of plates and provided by ASTM C1499-15 (2015) [29]:

$$\sigma_f = \frac{3F}{2\pi h^2}\left[(1-\nu)\frac{D_S^2 - D_L^2}{2D^2} + (1+\nu)\ln\frac{D_S}{D_L}\right] \tag{5}$$

where F is the maximum load, h and D are the thickness and the side of the glass plate, respectively, and ν is the Poisson's ratio. We tested 17 coated and 23 uncoated glass plates, in order to compare the results.

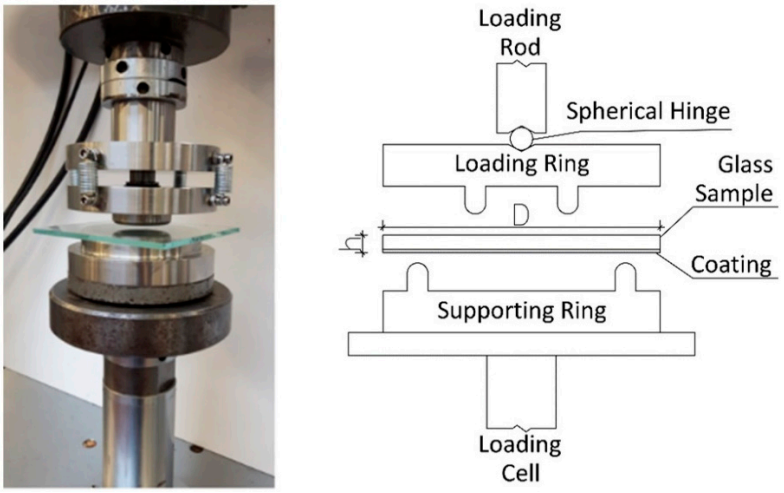

Figure 4. Coaxial double ring set-up for the mechanical load test.

3. Results and Discussion

3.1. Surface Treatment of Glass and Properties of the Coating

In order to prevent stress corrosion of glass, we developed a protective coating made with a cycloaliphatic acrylic resin copolymerized with a methacrylic perfluoropolyether (PFPE) and an acrylic silane primer, cured by UV-light, referred to as EFD (see Table 1).

The wettability and the surface energy of the coatings were estimated through water and hexadecane static contact angle measurements (see Equations (2) and (3)). The static contact angle values were 103.18° ± 1.58° and 52.10° ± 2.18° for water and hexadecane, respectively. The calculated surface energy was γ_s = 19.18 mN/m, with a polar component γ_s^P = 1.36 mN/m and a dispersive component γ_s^D = 17.92 mN/m. This value is much lower than the coating without fluorinated co-monomer and similar to the pure PFPE [23]. The obtained results indicated and confirmed that the presence of PFPE monomer in a small amount (1 phr) ensures a strong surface modification, because it is able to migrate to the surface exposed to air, creating a compositional profile in the coating as discussed in a previous work [30].

The surface roughness, measured according to DIN 4768, was similar for the bare glass slide and for the ED coating, while it was higher for the EFD coating. The FD coating could not be assessed as it was scratched by the stylus tip during the measurement. For the glass slide, the values obtained were R_a = 0.05 ± 0.005 µm, R_z = 0.3 ± 0.05 µm, and R_{max} = 0.3 ± 0.05 µm; for the ED coating, R_a = 0.06 ± 0.02 µm, R_z = 0.3 ± 0.05 µm, and R_{max} = 0.3 ± 0.1 µm; for the EFD coating, R_a = 0.21 ± 0.08 µm, R_z = 2.4 ± 1.1 µm, and R_{max} = 3.8 ± 2.3 µm.

UV-visible analysis was done on the EFD coating in order to evaluate its transparency, which is relevant to preserve the properties of glass. The results are shown in Figure 5, where they are compared to ED (formulation with only Ebecryl® 130 and Darocur® 1173) and FD (formulation with only Fluorolink® MD700 and Darocur® 1173) spectra taken from [23]. The transmittance is higher than 80% in the visible range for all the formulations, which means that the transparency of glass is almost completely preserved.

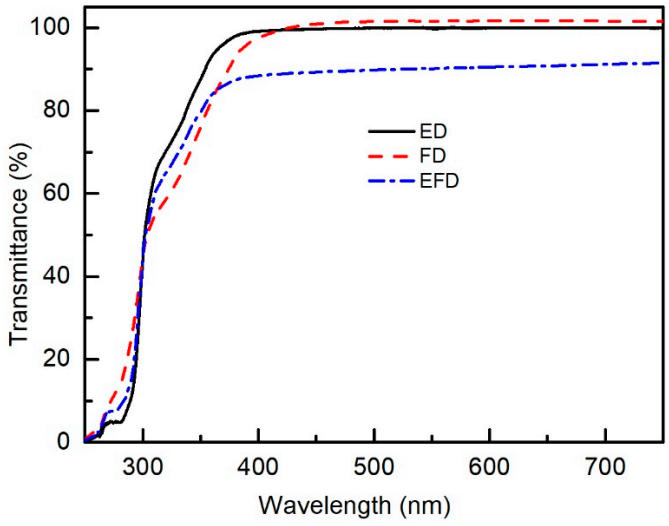

Figure 5. UV-visible (UV-VIS) spectra of ED, FD, and EFD coatings.

The gloss measurement revealed that when the ED coating was applied on the glass slides, the gloss increased by 5% with respect to the bare slide, while with the FD and EFD coatings, it decreased by 22% and 20%, respectively. This again suggests that the surface of the coating is enriched in the PFPE monomer, which is characterized by lower gloss values.

Barrier properties were assessed by $WVTR_{25}$ tests (as defined in Section 2.3), performed on the UV-cured films, and the results were compared to a polyethylene (PET) film, which showed $WVTR_{25}$

= 22.4 ± 0.45 g/(m^2·24 h). The $WVTR_{25}$ results are presented in Table 2. The coating made only of PFPE (FD) was very leaky, whereas the results of ED and EFD coatings were similar. Therefore, it was proven that the permeability to water of the coating is not affected by the presence of a small amount of fluorinated component. The $WVTR_{25}$ of the EFD film was of the same order of magnitude as the PET, showing acceptable barrier to water properties.

Table 2. Barrier to water results.

Composition	$WVTR_{25}$ g/(m^2·24 h)
EFD	87.1 ± 15.8
ED	53.1 ± 7.76
FD	316 ± 20.2

Before and after the permeability measurements, the films' morphology was observed with an optical microscope in order to find possible evidence of degradation due to the exposure to water vapor. A magnification of the EFD and FD film surfaces after the permeability tests is shown in Figure 6: The EFD film did not show significant damage, while on the FD surface, several pinholes were visible. The presence of pinholes in the coating is consistent with the high value of $WVTR_{25}$ obtained.

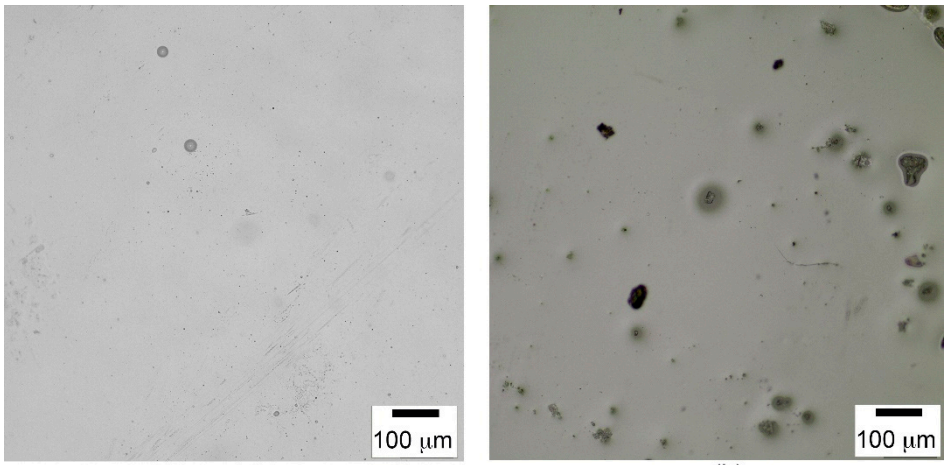

Figure 6. Surface of EFD (**a**) and FD (**b**) coatings after permeability test.

3.2. Adhesion Properties of the Coating

The adhesion properties between the photopolymerized coatings and glass were studied. In order to improve the adhesion between the glass substrate and the coatings, a silane coupling agent was used to functionalize the glass surface. A silane with an acrylic functional group was chosen, so that it could co-react with UV-cured coating, creating a covalent bond. Different concentrations of silane in different solvents were tested in order to select the most economical and environmentally friendly solution in view of a commercial application. Water contact angle was performed on untreated and silanized glass, as the successful modification of the glass surfaces is expected to significantly modify the surface's hydrophilic character [31]. As expected, the value obtained on the untreated glass slides was lower than 10°, confirming the full wettability of the raw substrates. The surface functionalization of glass with the silane increased the θ_w in all the tested conditions. Similar results were obtained with 1 vol.% silane in ethanol (θ_w = 69.4° ± 3.1°) and 0.2 vol.% silane in water (θ_w = 67.6° ± 4.1°). With 0.2 vol.% in ethanol, the contact angle was lower (θ_w = 56.6° ± 3.0°); therefore the silanization process in water was more efficient, which is relevant for economic and environmental sustainability reasons.

A preliminary assessment of adhesion was performed, checking the resistance upon immersion in water. The coatings were cured on untreated and silanized glass. Table 3 shows the results obtained after 14 days of immersion in water at RT, followed by 4 h of immersion at 60 °C: In the "coating failure" column, the time elapsed before the detachment of the coating from the glass substrate was reported. The coating detached from the untreated glass after 1 day at RT, whereas all systems with treated substrates survived the entire immersion test, confirming the effectiveness of the surface silanization in the improvement of adhesion and water resistance.

Table 3. Results of immersion test of coated glass with different silanization conditions.

Glass Surface Treatment	Coating Failure
None	1 day
Silanization 0.2 vol.% in ethanol	No
Silanization 1 vol.% in ethanol	No
Silanization 0.2 vol.% in water	No

Single lap shear tests (for which the geometry of the specimens and the set up are described in Section 2.3) were performed on EFD joints on silanized glass slides. The shear stress vs. displacement curves are reported in Figure 7 and the obtained average τ_{max} is reported in Table 4, together with the data regarding the inspection of the joints after failure. Also reported in the table are the data obtained for FD and ED, taken from [23]. The average value of τ_{max} obtained for EFD specimens was 24.9 ± 2.8 MPa, which proved a good adhesion between the glass substrate and the photopolymerized formulation. In the absence of silanization, it was not possible to perform the test because the adhesion was so poor that the glass slides detached during the preparation of the specimens. The values of τ_{max} are very similar for ED and EFD, while the reported τ_{max} for FD specimens is lower. The results proved that the small amount of the fluorinated component does not affect the adhesion properties of the coating, assuming that the PFPE chains migrate far from the glass surfaces. For all the specimens, the joint failed to leave the entire polymer disk on one side of the joint. The sites of the glass slides where the joint detached (detachment sites) were inspected with water contact angle measurements: For the ED and EFD joints, the water contact angle measurements gave similar results, and the measured value confirmed that the glass surfaces were still silanized. For the FD joints, the contact angle value was higher, which probably indicated a residual presence of the polymer.

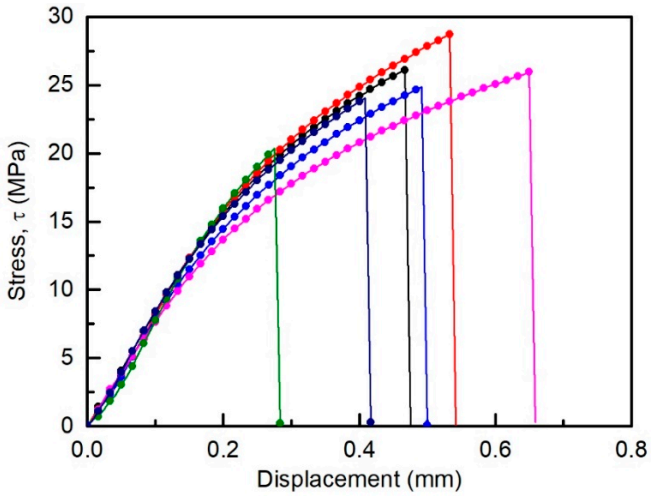

Figure 7. Stress–displacement curves obtained in the lap shear test for EFD joints on silanized glass: six specimens were tested and each line corresponds to one specimen.

Table 4. Results of lap shear test: τ_{max} is the shear strength, θ_w is the water contact angle measured on the glass surface at the joint detachment site right after the lap-shear test, and θ_w' is the water contact angle measured on the detachment site after rinsing.

Property	EFD	ED	FD
τ_{max} (MPa)	24.9 ± 2.8	24.5 ± 2.8	5.8 ± 1.0
θ_w (°)	68.4 ± 2.5	61.5 ± 2.6	75.1 ± 2.5
θ_w' (°)	65.8 ± 2.8	60.8 ± 2.4	72.6 ± 4.3

3.3. *Effect of the Coating on Glass Stress Corrosion Prevention*

In order to evaluate the effectiveness of the EFD coating in hindering stress corrosion, load tests were performed on glass plates immersed in water with the coaxial double ring setup (details are described in Section 2.3). Uncoated and coated glass plates were tested, and the values of equibiaxial tensile strength were found. Only one side of the glass plate was coated, i.e., the one subjected to tensile stresses during the coaxial double ring test (see Figure 4).

A typical load vs. plate deflection curve obtained from the load test is reported in Figure 8. As expected, the perfectly linear-elastic mechanical response is limited by a brittle failure, which determines a sudden and complete loss of the load carrying capacity.

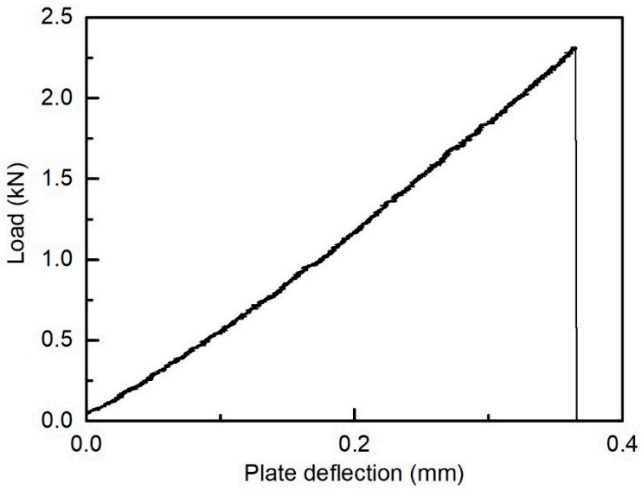

Figure 8. Coaxial double ring load test: Typical load–deflection curve.

Glass strength is highly dependent on the size of surface flaws. Therefore, a high dispersion of data is usually obtained, and a statistical analysis of the results is recommended. The distribution of the equibiaxial strength was analyzed in terms of the cumulative distribution function (CDF). Such a function provides the relative number of glass plates, N (σ_f), that fails for a strength lower or equal to σ_f (probability of failure). The CDFs are shown in Figure 9 for uncoated and coated specimens.

The data points are nicely fitted by the expression of the CDF, associated with the probability density function of the Gauss distribution:

$$f(\sigma_f) = \frac{1}{s\sqrt{2\pi}} \exp\left[-\frac{1}{2}\left(\frac{\sigma_f - \mu}{s}\right)^2\right] \quad (6)$$

where σ_f is the glass strength, and μ and s are the mean and the standard deviation, respectively. They are estimated according to the method of moments:

$$\mu = \frac{1}{n}\sum_{i=1}^{n} \sigma_{f,i} \quad (7)$$

and

$$s = \sqrt{\sum_{i=1}^{n} \frac{\left(\sigma_{f,i} - \mu\right)^2}{n-1}} \tag{8}$$

where n is the sample size.

The mean strength for uncoated specimens was 63.1 MPa, whereas that for coated specimens was 111.5 MPa. Therefore, the effectiveness of the photopolymerized coating was proven by an increase of the mean strength of about 76%. The standard deviations were very similar in the two cases, being 15.3 MPa for the uncoated specimens and 19.8 MPa for the coated specimens.

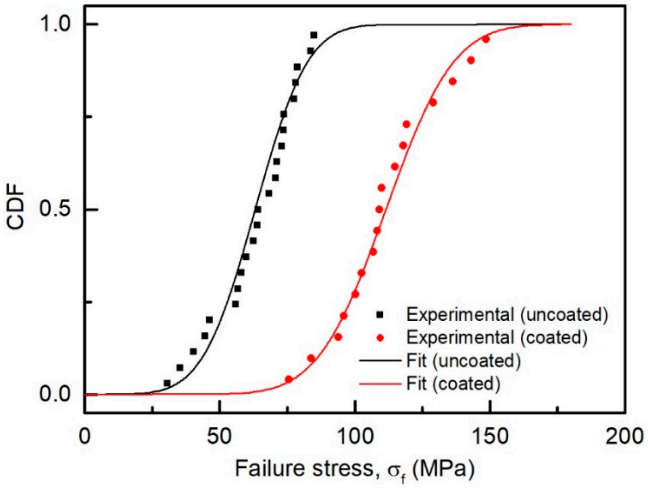

Figure 9. Cumulative distribution function (CDF) of the equibiaxial tensile strength for coated and uncoated glass plates.

4. Conclusions

A coating was prepared with a cycloaliphatic UV-curable resin, a fluorinated methacrylate co-monomer, a co-reactive silane primer, showing a good barrier to water vapor, hydrophobicity, transparency, and adhesion properties. It was successfully used to prevent stress corrosion, thus increasing the exploitable strength of glass. Good adhesion and high water repellency were present at the same time, thanks to a compositional gradient. The hydrophobic behavior was due to the presence of a low amount (1 phr) of the fluorinated co-monomer, which selectively enriched the outer surface of the coatings. The adhesion was due to the covalent bonding between the silane layer and the coating itself. The effectiveness of the coating was assessed with the coaxial double ring load test. Coated and uncoated glass plates were tested and an increment of 76% of the mean tensile strength was found for coated specimens.

In spite of the fact that the obtained results are very promising, also compared to previous experiences published in the literature [32], further work is needed before the developed coating can be used in real applications. A wider experimental investigation has to be carried out to investigate the effectiveness of the coating in glass stress corrosion prevention on different kinds of glass, including aged glass. Then, the coating durability is an important issue to be tackled. In this context, artificial weathering by exposing coated specimens to fluorescent UV lamps, heat, and water, and artificial ageing by means of sand abrasion will be considered.

Author Contributions: Conceptualization, R.B., M.C. and S.D.V.; Methodology, S.D.V. and M.C.; Investigation, G.M., S.D.V. and A.V.; Writing—Original Draft Preparation, S.D.V. and G.M.; Writing—Review and Editing, S.D.V., M.C., G.M., A.V. and R.B.; Supervision, R.B. and M.C.; Project Administration, M.C.; Funding Acquisition, M.C.

Funding: This research was funded by Politecnico di Torino and Compagnia di San Paolo within the programme "Create a network around your research idea".

Acknowledgments: The authors would like to thank Stefano Forzano and Luisa Gaiero for the specimen preparation, and Solvay Specialty Polymers for donating Fluorolink® MD700.

Conflicts of Interest: The authors declare no conflict of interest. The funders had no role in the design of the study; in the collection, analyses, or interpretation of data; in the writing of the manuscript, or in the decision to publish the results.

References

1. Bos, F.; Louter, C.; Veer, F. *Challenging Glass: Conference on Architectural and Structural Applications of Glass, Faculty of Architecture, Delft University of Technology, May 2008*; IOS Press: Amsterdam, The Netherlands, 2008; ISBN 978-1-58603-866-3.
2. Zarnic, R.; Tsionis, G.; Gutierrez Tenreiro, E.; Pinto Vieira, A.; Geradin, M.; Dimova, S. *Purpose and Justification for New Design Standards Regarding the Use of Glass Products in Civil Engineering Works*; JRC 037739; OPOCE: Luxembourg, 2007.
3. Rice, P.; Dutton, H. *Structural Glass*; Taylor & Francis: New York, NY, USA, 1995; ISBN 978-0-419-19940-3.
4. Haldimann, M.; Overend, M.; Luible, A. *Structural Use of Glass*; IABSE Association: Zurich, Switzerland, 2008.
5. Reddy, K.P.R.; Fontana, E.H.; Helfinstine, J.D. Fracture toughness measurement of glass and ceramic materials using chevron-notched specimens. *J. Am. Ceram. Soc.* **1988**, *71*, C310–C313. [CrossRef]
6. Soga, N. Elastic moduli and fracture toughness of glass. *J. Non-Cryst. Solids* **1985**, *73*, 305–313. [CrossRef]
7. Le Bourhis, E. *Glass: Mechanics and Technology*; Wiley-VHC: Weinheim, Germany, 2014.
8. Ast, J.; Ghidelli, M.; Durst, K.; Göken, M.; Sebastiani, M.; Korsunsky, A.M. A review of experimental approaches to fracture toughness evaluation at the micro-scale. *Mater. Des.* **2019**, *173*, 107762. [CrossRef]
9. Michalske, T.; Freiman, S. A molecular mechanism for stress-corrosion in vitreous silica. *J. Am. Ceram. Soc.* **1983**, *66*, 284–288. [CrossRef]
10. Ronchetti, C.; Lindqvist, M.; Louter, C.; Salerno, G. Stress-corrosion failure mechanisms in soda-lime silica glass. *Eng. Fail. Anal.* **2013**, *35*, 427–438. [CrossRef]
11. Alloteau, F.; Lehuédé, P.; Majérus, O.; Biron, I.; Dervanian, A.; Charpentier, T.; Caurant, D. New insight into atmospheric alteration of alkali-lime silicate glasses. *Corros. Sci.* **2017**, *122*, 12–25. [CrossRef]
12. Barlet, M.; Delaye, J.-M.; Boizot, B.; Bonamy, D.; Caraballo, R.; Peuget, S.; Rountree, C.L. From network depolymerization to stress corrosion cracking in sodium-borosilicate glasses: Effect of the chemical composition. *J. Non-Cryst. Solids* **2016**, *450*, 174–184. [CrossRef]
13. Pallares, G.; George, M.; Ponson, L.; Chapuliot, S.; Roux, S.; Ciccotti, M. Multiscale investigation of stress-corrosion crack propagation mechanisms in oxide glasses. *Corros. Rev.* **2015**, *33*, 501–514. [CrossRef]
14. Gy, R. Ion exchange for glass strengthening. *MSEB* **2008**, *149*, 159–165. [CrossRef]
15. Gao, Q.; Liu, Q.; Li, M.; Li, X.; Liu, Y.; Song, C.; Wang, J.; Liu, J.; Shen, G.; Han, G. Effect of glass tempering on microstructure and functional properties of SnO_2: F thin film prepared by atmosphere pressure chemical vapor deposition. *Thin Solid Films* **2013**, *544*, 357–361. [CrossRef]
16. Bongiovanni, R.; Vitale, A. Smart multiphase polymer coatings for the protection of materials. In *Smart Composite Coatings and Membranes*; Montemor, M.F., Ed.; Woodhead: Sawston, UK, 2016; pp. 213–234, ISBN 978-1-78242-283-9.
17. Corrigan, N.; Yeow, J.; Judzewitsch, P.; Xu, J.; Boyer, C. Seeing the light: Advancing materials chemistry through photopolymerization. *Angew. Chem. Int. Ed.* **2019**, *58*, 5170–5189. [CrossRef] [PubMed]
18. Vitale, A.; Bongiovanni, R.; Ameduri, B. Fluorinated oligomers and polymers in photopolymerization. *Chem. Rev.* **2015**, *115*, 8835–8866. [CrossRef] [PubMed]
19. Zhang, K.; Li, T.; Zhang, T.; Wang, C.; Wang, C.; Wu, M. Adhesion improvement of UV-curable ink using silane coupling agent onto glass substrate. *J. Adhes. Sci. Technol.* **2013**, *27*, 1499–1510. [CrossRef]
20. Yang, L.; Thomason, J. Effect of silane coupling agent on mechanical performance of glass fibre. *J. Mater. Sci.* **2013**, *48*, 1947–1954. [CrossRef]
21. Wang, Z.; Cousins, I.T.; Scheringer, M.; Hungerbühler, K. Fluorinated alternatives to long-chain perfluoroalkyl carboxylic acids (PFCAs), perfluoroalkane sulfonic acids (PFSAs) and their potential precursors. *Environ. Int.* **2013**, *60*, 242–248. [CrossRef] [PubMed]
22. Kotthoff, M.; Bücking, M. Four chemical trends will shape the next decade's directions in perfluoroalkyl and polyfluoroalkyl substances research. *Front. Chem.* **2018**, *6*, 103. [CrossRef]

23. Dalle Vacche, S.; Forzano, S.; Vitale, A.; Corrado, M.; Bongiovanni, R. Glass lap joints with UV-cured adhesives: Use of a perfluoropolyether methacrylic resin in the presence of an acrylic silane coupling agent. *Int. J. Adhes. Adhes.* **2019**, *92*, 16–22. [CrossRef]
24. Swentek, I.; Wood, J.T. Measuring polymer composite interfacial strength. *Compos. B* **2014**, *58*, 235–241. [CrossRef]
25. Wu, S. *Polymer Interface and Adhesion*; Marcel Dekker: New York, NY, USA, 1982; ISBN 978-0-8247-1533-5.
26. *DIN 4768:1990 Determination of Surface Roughness Values of the Parameters R_a, R_z, R_{max} by Means of Electrical Contact (Stylus) Instruments; Terminology, Measuring Conditions*; German Institute for Standardisation: Berlin, Germany, 1990.
27. *ASTM D870-15 Standard Practice for Testing Water Resistance of Coatings Using Water Immersion*; ASTM International: West Conshohocken, PA, USA, 2015.
28. *ASTM F372-99 Standard Test Method for Water Vapor Transmission Rate of Flexible Barrier Materials Using an Infrared Detection Technique*; ASTM International: West Conshohocken, PA, USA, 2003.
29. *ASTM C1499-15 Standard Test Method for Monotonic Equibiaxial Flexural Strength of Advanced Ceramics at Ambient Temperature*; ASTM International: West Conshohocken, PA, USA, 2015.
30. Bongiovanni, R.; Lombardi, V.; Priola, A.; Tonelli, C.; Di Meo, A. Surface properties of acrylic coatings containing perfluoropolyether chains. *Surf. Coat. Int. B: Coat. Trans.* **2003**, *86*, 53–57. [CrossRef]
31. Vistas, C.R.; Águas, A.C.P.; Ferreira, G.N.M. Silanization of glass chips—A factorial approach for optimization. *Appl. Surf. Sci.* **2013**, *286*, 314–318. [CrossRef]
32. Lindqvist, M.; Louter, C.; Lebet, J.-P. Edge-strengthening of structural glass with protective coatings. *Key Eng. Mater.* **2012**, *488–489*, 331–334. [CrossRef]